PLANETARY SCIENCE

Possible detection of hydrazine on Saturn's moon Rhea

Mark Elowitz[1]*, Bhalamurugan Sivaraman[2]*, Amanda Hendrix[3], Jen-Iu Lo[4], Sheng-Lung Chou[4], Bing-Ming Cheng[4†], B. N. Raja Sekhar[5], Nigel J. Mason[6]

We present the first analysis of far-ultraviolet reflectance spectra of regions on Rhea's leading and trailing hemispheres collected by the Cassini Ultraviolet Imaging Spectrograph during targeted flybys. In particular, we aim to explain the unidentified broad absorption feature centred near 184 nm. We have used laboratory measurements of the UV spectroscopy of a set of candidate molecules and found a good fit to Rhea's spectra with both hydrazine monohydrate and several chlorine-containing molecules. Given the radiation-dominated chemistry on the surface of icy satellites embedded within their planets' magnetospheres, hydrazine monohydrate is argued to be the most plausible candidate for explaining the absorption feature at 184 nm. Hydrazine was also used as a propellant in Cassini's thrusters, but the thrusters were not used during icy satellite flybys and thus the signal is believed to not arise from spacecraft fuel. We discuss how hydrazine monohydrate may be chemically produced on icy surfaces.

INTRODUCTION

Our knowledge of the geology and surface topography of Rhea, Saturn's second largest moon, has been greatly advanced by several flybys during the Cassini-Huygens mission. The surface of Rhea is heavily cratered with geomorphological features that indicate possible past endogenic activity, such as large impact craters that have undergone partial relaxation and extensional fault systems that are oriented in the north-south direction (*1*, *2*). Rhea's surface temperature ranges from about 40 to 100 K (*3*) and exhibits a high visible geometric albedo of 0.949 ± 0.003 (*4*). This albedo is consistent with a surface composed mostly of water-ice, a hypothesis supported by measurement of infrared (IR) absorption features (*5*). Rhea orbits Saturn at a radial distance of about 8.75 Saturn radii with a velocity of 8.5 km s^{-1}, which is much slower than the co-rotating plasma velocity of 86.3 km s^{-1}. Thus, the moon's trailing hemisphere (centered on 270°W) is irradiated by plasma traveling at ~57 km s^{-1}; E-ring grains also bombard and coat much of the surface of Rhea with a focus on the leading hemisphere (*6*). Such bombardment, from different sources, may lead to chemical changes in the irradiated surface and subsequent synthesis of a rich surface chemistry (*7*) while also explaining the chemical composition of Rhea's tenuous atmosphere of O_2 and CO_2 (*8*). However, the surface composition of Rhea's largely remains unknown (*9*). Here, we address the broad unidentified absorption band centered at 184 nm that was observed in far-ultraviolet (FUV) spectra recorded by Cassini-Ultraviolet Imaging Spectrograph (UVIS) during Rhea's flybys.

Rhea phase curves derived from Voyager disk-integrated and disk-resolved observations at a wavelength of 0.48 μm show an asymmetry in photometric properties between the leading and trailing hemispheres possibly due to differences in the Hapke roughness parameter between the leading and darker trailing hemisphere (*10*). An asymmetry between Rhea's brighter leading and darker hemisphere is also seen in the far ultraviolet (FUV) spectra acquired by the UVIS/FUV instrument on the Cassini spacecraft. A similar asymmetry between leading and trailing hemisphere seen in the phase curve and FUV reflectance spectra is also present in Saturn's other mid-sized icy satellites, Dione and Tethys (*11*). Cassini Imaging Science Subsystem (ISS) IR/Green/UV composite maps of Rhea, Dione, and Tethys also show an asymmetry between leading and trailing hemispheres (*9*). The darkening in the UV on these icy moons is plausibly caused by radiolytic reactions due to a corresponding asymmetry in irradiation by energetic particles of Saturn's magnetosphere (*12*). Molecules present in ice phase can be dissociated by such radiation, which can lead to the formation of different molecules that absorb in FUV, including an absorber centered at 184 nm.

Cassini UVIS observations and the 184-nm band

In this study, we use four Cassini UVIS/FUV disk-resolved observations of Rhea. The locations of the observations are shown in Fig. 1 with the observational geometry outlined in Table 1. The observations sample regions on the leading (yellow and blue slit field of views), trailing (green slit field of view), and anti-Saturnian (cyan slit field of view) hemispheres on Rhea. The UVIS spectra from the four observations of Rhea are shown in Fig. 2. To reduce noise in the UVIS data, a Savitzky-Golay smoothing filter was applied to each UVIS spectrum (*13*, *14*). Tests using Savitzky-Golay smoothing procedure showed it to perform better than basic smoothing filters based on box averaging and running means. All spectra are dominated by water-ice as indicated by the steep spectral slope centered near 165 nm, with a strength that depends on the abundance of water-ice and a wavelength that is dependent on the size of the ice grains and degree of minor contaminants. However, spectra also show a broad, weak absorption feature from approximately 179 to 189 nm, centered near 184 nm. This absorption feature has been noted in previous observations of other icy satellites [e.g., Phoebe (*15*)] in the Saturnian system, but, to date, its origin has not been explained satisfactorily (*15*). Attempts to fit Phoebe's 184-nm absorption feature, using various mixtures of tholin and ice, water-ice and carbon, water and kerogen, and water plus hydrogen cyanide (*15*), have proven to be unsuccessful. Royer *et al.* (*16*) discuss the 184-nm feature and point out its appearance, in some (but not all) observations of Mimas, Enceladus, Tethys, and Rhea. Therefore, in this work, we explore explanations for the broad absorption seen over the wavelength range of ~179 to 189 nm in UVIS spectra of Rhea.

[1]Department of Physical Sciences, The Open University, Milton Keynes MK7 6AA, UK. [2]Atomic Molecular and Optical Physics Division, Physical Research Laboratory, Ahmedabad 380 009, India. [3]Planetary Science Institute, Pasadena, CA 91106, USA. [4]National Synchrotron Radiation Research Center, Hsinchu, Taiwan. [5]B-1, Indus-1, Atomic and Molecular Physics Division, Bhabha Atomic Research Centre at RRCAT, Indore, India. [6]School of Physical Sciences, The University of Kent, Canterbury CT2 7NH, UK. *Corresponding author. Email: elowitzr@earthlink.net (M.E.); bhala@prl.res.in (B.S.) †Present address: Department of Medical Research, Hualien Tzu Chi Hospital, Buddhist Tzu Chi Medical Foundation, Hualien 970, Taiwan.

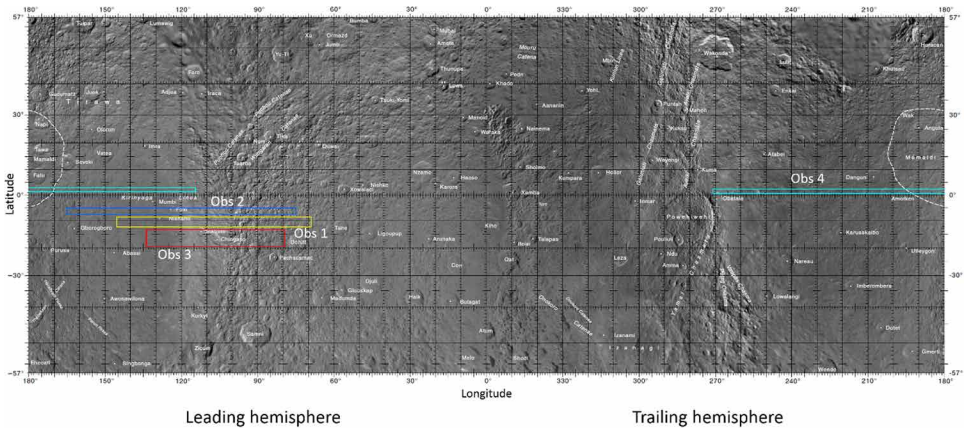

Fig. 1. Location of the four Cassini UVIS/FUV observations analyzed in this paper. UVIS observations sample Rhea's leading and trailing hemispheres. Each slit field of view represents 64 spatial pixels of the detector. Area within each box represents the integrated sum of all 64 detector rows, over all phase angle ranges.

Table 1. Table of Cassini UVIS observations presented in this paper. In the table, Lat1 and Lat2 are the latitude boundaries of the instrument footprint, Long1 and Long2 are the longitude boundaries, Phase is the phase angle (°), Incidence and Emission are the incidence and emission angles of the UVIS observation, and Range is the distance above the target surface on Rhea (in kilometers). The first and second rows for each observation list the start and end times of observation, respectively.

Obs.	Year	Day	Time	Lat1	Lat2	Long1	Long2	Phase	Incidence	Emission	Range
1	2007	242	01:43:35	−12.20	−8.53	68.80	145.16	20.6–23.1	1.9–61.2	12.9–81.5	11,169–11,783
	2007	242	01:44:35								
2	2007	242	01:54:23	−7.90	−5.06	75.26	165.48	26.1–28.9	5.2–56.1	8.3–82.8	14,952–15,599
	2007	242	01:55:23								
3	2007	242	01:35:31	−19.7	−13.2	79.55	134.27	17.0–18.4	2.6–50.3	18.9–63.5	8673–9312
	2007	242	01:37:31								
4	2011	011	06:04:38	1.10	2.62	115.50	271.37	14.5–16.4	6.4–91.2	3.0–80.4	34,060–35,583
	2011	011	06:08:38								

RESULTS

Using laboratory spectra to model Cassini UVIS observations

During the course of this work, we measured laboratory spectra of several molecular species (see table S1) and their mixtures to derive optical constants for use in Hapke modeling of mixtures. Limited phase cover observations did not permit a satisfactory derivation of Hapke parameters needed to produce model spectra. Instead, attempts to use limited phase angle coverage resulted in a wide range of Hapke parameters that fit UVIS phase curve data equally well within statistical error of the data. Solutions based on Hapke model results can be nonunique when photometric measurements are too sparse. In other words, the phase angle data available for Rhea are too limited in their coverage to constrain Hapke parameters (e.g., coherent backscatter opposition, asymmetry of the phase function of the ice grains, and macroscopic roughness parameter). As a result of these aforementioned problems, an alternative methodology was used to obtain Hapke parameters.

Since Rhea and Dione share similar geomorphology, based on Cassini high-resolution ISS imagery, and both mid-sized icy satellites have O_2/CO_2 exosphere (*8*, *17*), it is assumed that these two satellites have similar compositional and photometric properties. Both Rhea and Dione exhibit brighter leading hemispheres and show very little limb darkening at low phase angles (*18*). Brighter hemispheres are most likely caused by a deposition of pure water-ice from Saturn's E-ring (*19*) and both Rhea and Dione have similar photometric properties (based on similarities in the shape of the phase curves) and orange/violet color ratios, implying similar surfaces. Therefore, we chose to use Hapke parameters derived for Dione's leading hemisphere (*11*). The asymmetry parameter for the width of the forward and backward scattering lobes, and the relative amplitude of the scattering lobes is denoted by b and c, respectively, where $b = 0.35$ and $c = 1.0$. The roughness parameter (in radians) is denoted by S. The terms h and $B0$ characterize the shadow-hiding opposition surge, where $h = 0.457$ and $B0 = 0.95$.

Resultant model spectra of hydrazine monohydrate ($N_2H_4.H_2O$) and trichloromethane ($CHCl_3$) below a layer of water-ice approximately 0.125 μm thick are shown in Fig. 2 with the UVIS spectra. Spectral models using $N_2H_4.H_2O$, $CHCl_3$ below water-ice, and CCl_4 below water-ice were created using laboratory absorbance measurements and Hapke theory (*15*). The amount of non–water-ice component was 5%. For reference, a model of pure water-ice is also shown in the comparison plots (Fig. 2).

Examination of the modeled spectra in Fig. 2 clearly shows that $N_2H_4.H_2O$ or simple chloromethane molecules could explain the weak, broad absorption seen between approximately 179 and 189 nm. To

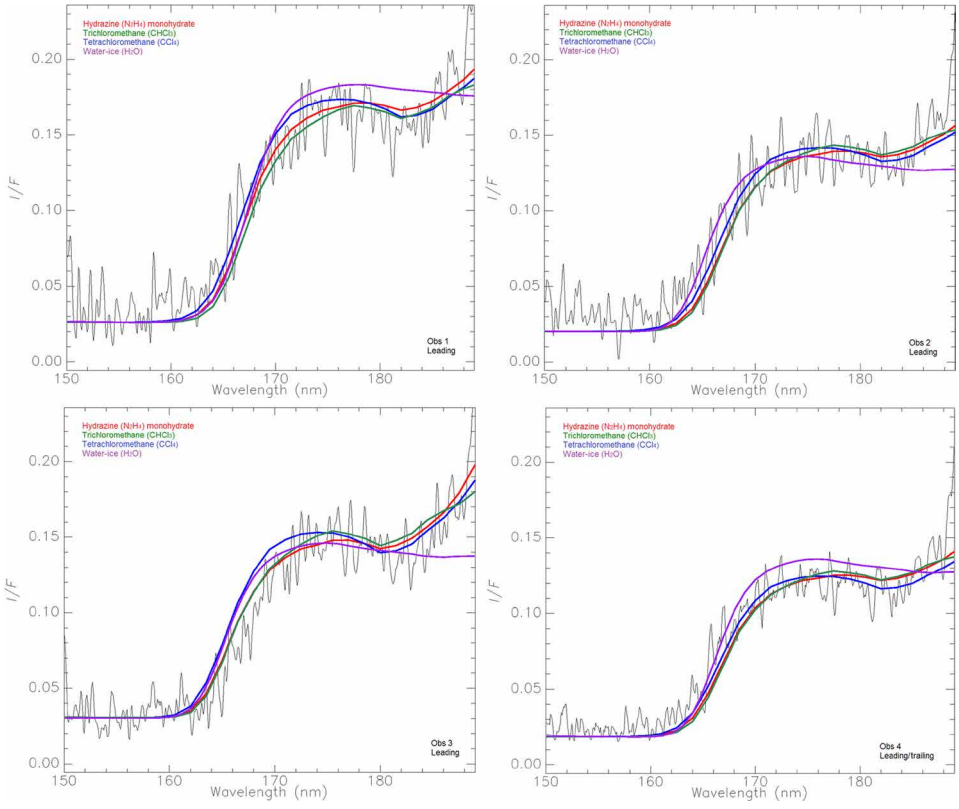

Fig. 2. UVIS-measured reflectance spectra (black spectra) of Rhea from the four observations shown in shown in Fig. 1 and Table 1. Spectral models are based on laboratory thin-ice measurements of the absorbance of two chloromethane compounds and $N_2H_4.H_2O$. Measurements were acquired at a temperature of 70 K under near-vacuum conditions to simulate surface environment of Rhea. Grain size used in the model spectra was 3 μm, and path length was set to 0.125 μm for Obs 1, 2, and 3, and 0.250 μm for Obs 4. Error, ±6% for the observational data, not added to spectra for clarity.

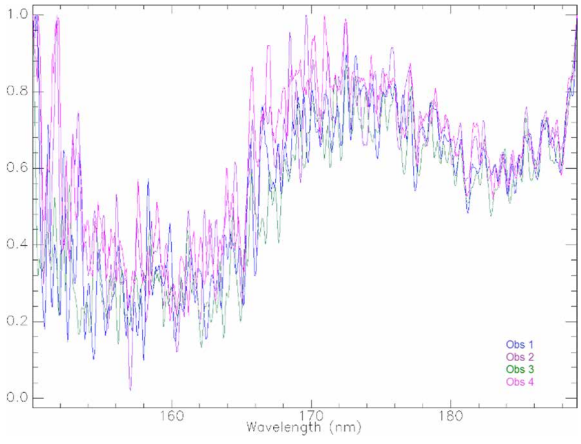

Fig. 3. Continuum-removed spectra showing the relative depth of the 184-nm absorption feature and relative positions of water-ice absorption edge. Within error limits of UVIS data, we detect no significant differences in the strength of the 184-nm absorption feature as a function of location on Rhea's surface. A minor change in the position of UV absorption edge due to water-ice is noted. The minor shift may be the result of different ice grain sizes and/or minor contaminants within the ice matrix. Error, ±6%, not added to spectra for clarity.

compare the relative strengths of absorption, we remove the continua of each spectrum to show four normalized spectra of Rhea. These results are shown in Fig. 3. We do not see any significant variation in the band strength with observation or location on Rhea.

DISCUSSION

To determine which chemical compound ($N_2H_4.H_2O$ or simple chlorine compounds) may be responsible for producing weak absorption from ~179 to 189 nm, we explore possible sources and sinks of each molecular species. Results of the modeling imply that the best agreement between the derived observational UVIS spectra and the modeled spectra occurs (i) with a chlorine-containing ice layer located just below a (~125 nm) layer of water-ice or (ii) when hydrazine is mixed with water in the form of a monohydrate. H_2O and CCl_4 are immiscible, because CCl_4 cannot form hydrogen bonds to water. On Rhea, there might be a source for CCl_4 (e.g., endogenic), with, at a later time, a fresh layer of water-ice being delivered on top of the CCl_4 from Saturn's E-ring. Since E-ring material could coat both hemispheres of Rhea, it would explain why CCl_4 below water-ice is seen in all UVIS spectra analyzed in this research. We obtain an equivalent thickness of water-ice of ~1.2×10^{-10} m/year or about 1.2×10^{-4} μm/year. Since UV reflectance spectroscopy is sensitive to only the upper few micrometers, we see that a layer of chloromethane compounds beneath a deposited water-ice could be readily detectable.

However, chlorine compounds are somewhat difficult to explain via chemical pathways, and their origin on Rhea would require the presence of an internal ocean layer or exogenic delivery by micrometeoroids and/or asteroids that contain chlorine. It should also be noted that $CHCl_3$ and CCl_4 have melting points of 209.7 and 250.2 K, respectively. Thus, if these compounds exist deep in the interior of

Rhea, they would depress the freezing point of water-ice increasing the probability of an aqueous layer. Chlorine-based salts (e.g., NaCl) have been detected in plumes of Enceladus (*20*), which provide evidence for an internal ocean; however, it is not likely that chlorine compounds could migrate to the surface of Rhea through cracks in the ice shell (assuming Rhea is partially differentiated) owing to the great depth of such a liquid layer as determined through numerical models (*21*). The only other possible source of chlorine is via exogenic delivery by chondritic asteroids over the history of Rhea. Condensed chlorine compounds on Rhea's surface could be redistributed to other regions of the satellite by sputtering induced by charged particles from Saturn's magnetosphere. This could, in turn, explain wide distribution of chlorine compounds as sampled by UVIS observations. Distribution of the observed chlorine species across Rhea's surface, in theory, should be determined by velocity distribution of sputtered molecules. If chlorine is delivered to the surface of Rhea, then it might be possible for free radical halogenation to occur via irradiation of UV photons and/or charged particles. This process could lead to molecular compounds with increased chlorination.

The main unresolved questions on this scenario is whether there are any barriers to these reactions at the lower temperatures encountered on the surface of Rhea. Furthermore, there is no evidence of CH_4 trapped within the ice matrix on Rhea. To synthesize CCl_4, the hydrogen in CH_4 has to be replaced by Cl and HCl is the byproduct in every step of replacing one hydrogen atom. Since HCl is also produced in the production of simple chloromethane compounds, it should also be present in the surface ice on Rhea. However, comparisons of the UVIS observations presented in this paper with laboratory thin ice measurements of deuterium chloride (DCl) (Fig. 4) suggest that no HCl is present on Rhea. Furthermore, production of CO_2 is also unlikely since it would require the presence of CCl_4. For these reasons, the focus of the remainder of this paper will be exploring the possible sources of $N_2H_4.H_2O$ on Rhea.

The production of $N_2H_4.H_2O$ is easier to explain than the presence of any chlorine-containing derivatives as it can be produced in chemical reactions involving water-ice and ammonia, or possibly delivered from Titan's nitrogen-rich atmosphere where the compound could be synthesized. The possibility of contamination of the UVIS data by a hydrazine propellant from Cassini spacecraft was considered but we feel is highly unlikely, since the hydrazine thrusters were not used during icy satellite flybys. Furthermore, there are numerous observations of all icy Saturnian satellites that do not show the 184-nm feature. For instance, several disk-integrated spectra acquired from Tethys show no indication of absorption near 184 nm (Fig. 5). Furthermore, a calibration UVIS/FUV spectrum of the star epsilon CMa was obtained during the T41 I occultation on 23 February 2008 (*22*). The spectrum shows no indication of a broad absorption feature between ~179 and 189 nm. Thus, the presence of such a 184-nm feature is confirmed as being specific to Rhea surface observations by the Cassini spacecraft and is not a result of contamination from hydrazine fuel on the UV spectrometer.

Irradiation of ammonia by charged particles from Saturn's magnetosphere may induce dissociation of NH_3 molecules to synthesize N_2H_2 and N_2H_4. Lyman alpha photons with an energy of 10.2 eV (121.6 nm) can also dissociate NH_3, leading to the production of N_2H_4 (*23*). The possibility of hydrazine synthesis in Titan's atmosphere has also been investigated in laboratory experiments carried out by Zheng *et al.* (*24*). The team performed laboratory experiments to investigate synthesis of hydrazine from irradiation of NH_3 ice over a temperature range of 10 to 60 K, where two NH_2 radicals from NH_3 dissociation synthesize N_2H_4. Initial IR spectrum could not identify absorption bands due to N_2H_4 spectra overlapping NH_3 features. However, during the warm-up phase of the experiment, hydrazine absorption features became visible in the IR spectrum. The experiment conducted by Zheng *et al.* (*24*) showed that strength of hydrazine absorption bands increases as ammonia sublimates.

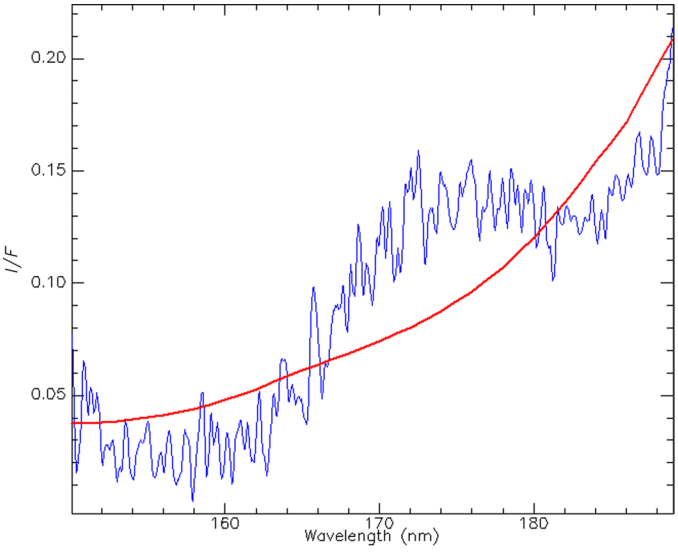

Fig. 4. Deuterium chloride spectrum compared with a Rhea FUV spectrum. Error, ±6% for the observational data and ±5% for the experiment data, not added to spectra for clarity.

The source of NH_3 could be primordial, incorporated into the interior of Rhea during its formation and brought to surface during a period when Rhea had endogenic activity. Evidence for past regional endogenic activity on Rhea is apparent in Cassini ISS imagery in the form of morphological features, including relaxation of large impact craters, curvilinear grabens, and orthogonal ridges. In contrast, transfer of the ammonia observed in plumes of Enceladus to Rhea's surface is unlikely due to Rhea's distance from Enceladus and the instability of NH_3 to photo- and radiolytic dissociation. If Rhea is a uniform mixture of rock and ice (undifferentiated), then minor amounts of ammonia may be present over a large percentage of its surface. This would explain why hydrazine appears to be present over a geographically wide area as sampled by the UVIS observations. However, NH_3 is unlikely to survive on the surface of Rhea indefinitely. Furthermore, there are several processes that can reduce production rate or prevent synthesis of hydrazine within the upper surface ice layer of Rhea.

Since water-ice is most likely to host NH_3 ice, the probability of UV photons, with energy 10.2 eV (121.6 nm) or less, destroying NH_3 decreases because of the strong absorption of Lyman-alpha photons by the water-ice matrix. This scenario applies for the case where NH_3 is located beneath water-ice, and the photon path length is short enough to allow sampling by UV/IR spectroscopy. Other impurities, such as hydrazine or chlorine, may also be shielded against destruction by UV photons beneath a thin layer of water-ice. Lower-energy (<6.05 eV or <205 nm) radiation, however, can penetrate further into the surface ice layer, with the potential to destroy any underlying impurities, such as NH_3, chlorine, and hydrazine compounds. Instability due to longer wavelength photons may explain why no

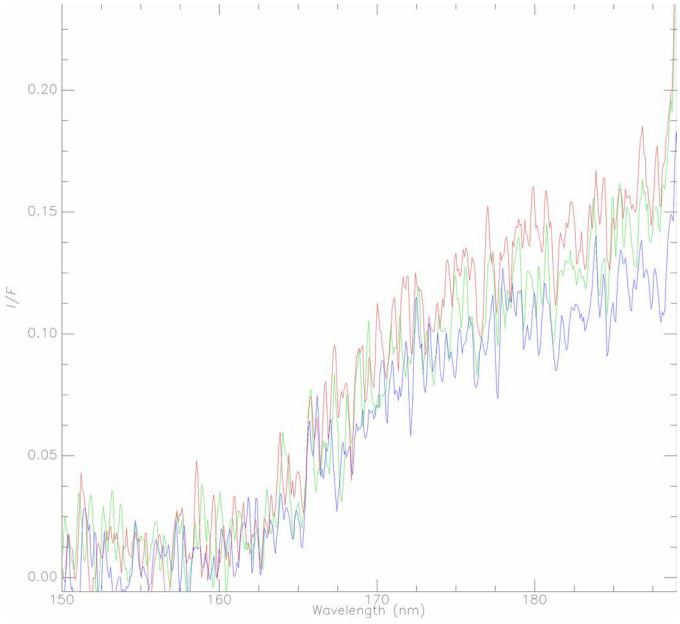

Fig. 5. Cassini UVIS/FUV disk-integrated spectra of trailing hemisphere of Saturn's icy moon Tethys acquired during 2015. Observations were collected at a phase angle of ~29°. All three spectra are dominated by water-ice as indicative of steep FUV drop-off between ~160 and 170 nm. None of the spectra show the presence of the 184-nm absorption feature that is seen in FUV spectra of Rhea. Error, ±6%, not added to spectra for clarity.

NH_3 has been detected on Rhea over the wavelength range sampled by Cassini UVIS instrument. Ammonia could, in theory, be more stable if it exists on icy satellites in the form of a hydrate mixture—i.e., ammonia in the form of a hydrate will minimize energy in thermodynamic equilibrium. Concentration of any hydrazine synthesized in chemical reactions between NH_3 and H_2O will depend on several factors, including dissociation rate of NH_3 by energetic electrons from Saturn's magnetosphere and localized heating due to micrometeoroid bombardment. Localized heating will tend to bring fresh NH_3 to the surface, where it is susceptible to destruction by radiolysis. NH_3 sublimation due to localized heating can also occur since NH_3 is more volatile than water-ice. For these reasons, we look for an exogenic source of hydrazine. A possible exogenic source of hydrazine would be from another moon of Saturn with an atmosphere capable of synthesizing the chemical compound.

Saturn's largest satellite Titan orbits at approximately 20 Saturnian radii (exterior to Rhea) with an orbital period of 15.95 days. Titan's thick atmosphere is dominated by N_2 with minor amounts of hydrocarbons including CH_4. If N_2 (or N_2H_4, since 4H does not add a significant atomic mass to the hydrazine molecule) can escape from Titan's atmosphere, then it is possible that Rhea could accumulate it as it orbits Saturn. Rough estimates show that Jean's escape mechanism is not sufficient to eject hydrazine from Titan's atmosphere. Thus, an alternative ejection mechanism is required to eject N_2H_4 from Titan's atmosphere. Sputtering is a nonthermal process that is an effective escape mechanism on small solar system bodies (e.g., Titan and Mars) that have no inherent magnetic fields. Experiments conducted by De La Haye *et al.* (*25*) lead to a sputtering rate for N_2 on Titan of ~3.6×10^{28} atomic mass units/s (59.78 kg/s). Thus, over a geological timespan of 4 billion years, the amount of N_2 ejected from Titan's atmosphere due to sputtering would be ~7.5×10^{18} kg or 5.6×10^{-5} Titan masses. This is equivalent to the mass of some of the more massive asteroids. It is also important to note that this is an upper limit estimate that assumes that N_2 or N_2H_4 has existed in Titan's atmosphere over the last 4 billion years and that it does not get destroyed before being accumulated onto Rhea's surface. We should, however, note that Rhea's surface temperature is not supportive to harbor pure N_2 or CH_4 to remain on the surface; however, they may be present in low concentration in water-ices but because of the low absorption cross section of the N_2 and CH_4 absorption band coinciding with the water absorption below 145 nm (*26*), we are unable to conclude the presence of these molecules in the FUV spectra. Future research work on the details associated with the production, ejection, and transfer of hydrazine from Titan's atmosphere are, therefore, needed to assess whether satellite-to-satellite transfer of materials can explain the possible presence of $N_2H_4.H_2O$ on Rhea, and why the feature appears in the spectra of some satellites sometimes, and not others [e.g., (*16*)].

The first detailed geochemical survey of Rhea's icy surface in the FUV region indicates the possible presence of chloromethane compounds under a layer of water-ice or the presence of a $N_2H_4.H_2O$ complex. The presence of CCl_4 or $CHCl_3$ beneath a thin layer of water-ice is more difficult to explain, and we therefore suggest that $N_2H_4.H_2O$ is the more likely candidate for the observed UV spectral feature at 184 nm, since it can be produced by chemical reactions induced by irradiation processes on molecular ices containing water and ammonia. If ammonia is present within the icy upper layer on Rhea, then the source of $N_2H_4.H_2O$ might be indigenous in nature. It is also possible that hydrazine could be synthesized in the atmosphere of Saturn's largest moon Titan and transferred to Rhea over geological timespans.

MATERIALS AND METHODS

Observations and data reduction

The Cassini UVIS is a spatial-spectral instrument (1024 spectral channels and 64 spatial elements) used to collect UV data over two spectral channels. The extreme UV and FUV channels cover the wavelength ranges of 56 to 118 nm and 110 to 190 nm, respectively, providing spectral resolutions of 0.24 and 0.48 nm. The entire slit length is 64 mrad. The Rhea spectra discussed here were collected using the FUV channel, and we focus on the ~150- to 190-nm region for the geochemical study of Rhea's surface since shorter wavelengths did not have sufficient signal-to-noise ratio (SNR) to allow chemical analysis.

Cassini UVIS/FUV datasets for the Rhea 2007, 2010, and 2011 targeted flybys were extracted from the NASA PDS archive. One constraint used in selecting the datasets is that the instrument footprint is completely filled with Rhea's surface. Another constraint is selecting the highest signal-to-noise spectra over the leading and trailing hemispheres of Rhea to provide the best chance of fitting model spectra. A table of the Cassini UVIS observations presented in this paper is listed in Table 1.

Each UVIS raw spectrum is converted to geophysical units by applying a unique set of calibration matrix coefficients to the data (*27*). All UVIS observations are corrected for background signals from the Cassini spacecraft radioisotope thermoelectric generators. The SNR of the calibrated spectra is increased by summing over a given number of spatial elements. Each calibrated spectrum is then converted to I/F (reflectivity) by dividing by a solar spectrum (scaled to the heliocentric distance of Rhea) obtained from the SOLSTICE

instrument on the SORCE spacecraft (*28*) for the given date of the UVIS observation, corrected for sub-solar longitude. The *I*/*F* spectrum can be mathematically expressed by

$$\frac{I}{F} = \frac{P}{(S/\pi)}$$

where *P* is the calibrated UVIS spectrum and *S* is the solar flux spectrum (scaled to the heliocentric distance of Rhea on the date of the observation), where $S = \pi F$. Each *I*/*F* spectrum is smoothed using a running mean method to reduce noise and allow easier comparisons with laboratory reference spectra.

The average SNR of the UVIS data presented in this work was calculated using a statistical method that is robust with respect to the presence of any outliers. The method does not depend on assumptions and/or decisions made by the user, since the signal is the median of the reflectance, and the noise calculation is based on the standard deviation of a Gaussian assuming a normally distributed variable. An advantage of this method is the simplicity used in the algorithm for calculating the SNR, which outweighs the slight increase in precision used by methods that depend on full information about the specific sensor. Since the method is generic in nature, the SNR calculated for spectra can be compared across different instruments. According to the Spectrum Data Model of the International Virtual Observatory Alliance, the statistical method used to calculate the SNR of the UVIS data is becoming the standardized method of computing the SNR of spectral data. For the UVIS observations presented in this paper, the average SNR is approximately 8.8 (near 180 nm). This SNR is approximately the same for all observations.

To determine the location of the UVIS instrument footprints on Rhea's surface, JPL NAIF SPICE (Space Planet Instrument Camera-matrix Events) kernels were used to calculate the relative positions of the Cassini spacecraft and Rhea, the orientation of the spacecraft and Rhea, and instrument pointing data at the time of each observation. The projection of the UVIS/FUV slit on Rhea's surface was plotted using the "Geometer" software, developed by the Cassini UVIS instrument team. The latitude and longitude calculated by the Geometer IDL code is used to produce an image of Rhea's surface with a projection of the UVIS instrument footprint for the observations presented in this paper. The "Environment for Visualization of Images" software package was used to produce the final UVIS/FUV slit field-of-view plots.

Experimental methodology

Experiments simulating Rhea conditions were carried out in an ultrahigh-vacuum chamber housing a cold finger on which a lithium fluoride (LiF) window was attached. The chamber pressure went down to 5×10^{-9} mbar while temperatures down to 10 K were achieved at the LiF window. This entire system was attached to the end station of the 03A1 High Flux beamline at the National Synchrotron Radiation Research Center (NSRRC), Taiwan. Vacuum UV (VUV) light in the 110- to 200-nm range was used to probe the molecular ices that are formed at low temperatures. To obtain the photoabsorption spectra of simulated molecular ices, a spectrum of the LiF window, *Io*, was recorded at 10 K. Then, after sample deposition, another spectrum was recorded, *I*. The photoabsorption spectrum was then obtained using the Beer-Lambert law.

Molecules from liquid samples of hydrazine monohydrate, trichloromethane, tetrachloromethane, and water were extracted into the gas phase before the gases were allowed into the chamber to form molecular ice films. In the case of layered ices, trichloromethane and tetrachloromethane were first deposited, respectively, above which water molecules were deposited, whereas in the case of mixed ices, a 1:1 mixture of tricholoromethane/tetrachloromethane with water was prepared in the gas phase before deposition. All the samples were deposited at 10 K and were later warmed to higher temperatures (mostly covering Rhea diurnal temperatures) for spectral recording. Apart from the molecules given above, we have compared the known VUV spectra of various astrochemical ices (table S1) (*26*, *29*–*38*) with that of the Rhea spectra.

SUPPLEMENTARY MATERIALS

Supplementary material for this article is available at http://advances.sciencemag.org/cgi/content/full/7/4/eaba5749/DC1

REFERENCES AND NOTES

1. J. M. Moore, P. M. Schenk, in *Lunar and Planetary Science Conference XXXVIII* (2007).
2. R. J. Wagner, G. Neukum, B. Giese, T. Roatsch, U. Wolf, in *Lunar and Planetary Science Conference XXXVIII* (2007).
3. C. J. A. Howett, J. R. Spencer, J. Pearl, M. Segura, Thermal inertia and bolometric Bond albedo values for Mimas, Enceladus, Tethys, Dione, Rhea and Iapetus as derived from Cassini/CIRS measurements. *Icarus* **206**, 573–593 (2010).
4. A. Verbiscer, R. French, M. Shuwalter, P. Helfenstein, Enceladus: Cosmic graffiti artist caught in the Act. *Science* **315**, 815 (2007).
5. U. Fink, H. P. Larson, T. N. I. Gautier III, R. R. Treffers, Infrared spectra of the satellites of Saturn—Identification of water ice on Iapetus, Rhea, Dione, and Tethys. *Astrophys. J.* **207**, L63–L67 (1976).
6. A. R. Hendrix, T. A. Cassidy, G. M. Holsclaw, C. Paranicas, C. J. Hansen, in *EPSC-DPS Joint Meeting* (2011), vol. 6, pp. 1638.
7. A. R. Hendrix, G. Filacchione, C. Paranicas, P. Schenk, F. Scipioni, Icy Saturnian satellites: Disk-integrated UV-IR characteristics and links to exogenic processes. *Icarus* **300**, 103–114 (2018).
8. B. D. Teolis, J. H. White, Dione and Rhea seasonal exospheres revealed by Cassini CAPS and INMS. *Icarus* **272**, 277–289 (2016).
9. P. Schenk, D. P. Hamilton, R. E. Johnson, W. B. McKinnon, C. Paranicas, J. Schmidt, M. R. Showalter, Plasma, plumes and rings: Saturn system dynamics as recorded in global color patterns on its midsize icy satellites. *Icarus* **211**, 740–757 (2011).
10. A. J. Verbiscer, J. Veverka, Albedo dichotomy of Rhea: Hapke analysis of Voyager photometry. *Icarus* **82**, 336–353 (1989).
11. E. M. Royer, A. R. Hendrix, First far-ultraviolet disk-integrated phase curve analysis of Mimas, Tethys and Dione from the Cassini-UVIS data sets. *Icarus* **242**, 158–171 (2014).
12. G. Strazzulla, A. C. Castorina, M. E. Palumbo, Ion irradiation of astrophysical ices. *Planet. Space Sci.* **43**, 1247–1251 (1995).
13. P. A. Gorry, General least-squares smoothing and differentiation by the convolution (Savitzky-Golay) method. *Anal. Chem.* **62**, 570–573 (1990).
14. A. Savitzky, M. J. E. Golay, Smoothing and differentiation of data by simplified least squares procedures. *Anal. Chem.* **36**, 1627–1639 (1964).
15. A. R. Hendrix, C. J. Hansen, Ultraviolet observations of Phoebe from the Cassini UVIS. *Icarus* **193**, 323–333 (2008).
16. E. M. Royer, L. W. Esposito, J. P. Elliott, Mapping of the 185nm absorption feature on the icy satellites of Saturn, in *Lunar and Planetary Science Conference L*, (2019).
17. B. D. Teolis, G. H. Jones, P. F. Miles, R. L. Tokar, B. A. Magee, J. H. Waite, E. Roussos, D. T. Young, F. J. Crary, A. J. Coates, R. E. Johnson, W.-L. Tseng, R. A. Baragiola, Cassini finds an oxygen–carbon dioxide atmosphere at Saturn's icy Moon Rhea. *Science* **330**, 1813–1815 (2010).
18. B. Buratti, J. Veverka, Voyager photometry of Rhea, Dione, Tethys, Enceladus and Mimas. *Icarus* **58**, 254–264 (1984).
19. C. J. A. Howett, J. R. Spencer, T. Hurford, A. Verbiscer, M. Segura, Thermophysical property variations across Dione and Rhea. *Icarus* **241**, 239–247 (2014).
20. F. Postberg, S. Kempf, J. Schmidt, N. Brilliantov, A. Beinsen, B. Abel, U. Buck, R. Srama, Sodium salts in E-ring ice grains from an ocean below the surface of Enceladus. *Nature* **459**, 1098–1101 (2009).
21. H. Hussmann, F. Sohl, T. Spohn, Subsurface oceans and deep interiors of medium-sized outer planet satellites and large trans-neptunian objects. *Icarus* **185**, 258–273 (2006).
22. T. T. Koskinen, R. V. Yelle, D. S. Snowden, P. Lavvas, B. R. Sandel, F. J. Capalbo, Y. Benilan, R. A. West, The mesosphere and lower thermosphere of Titan revealed by Cassini/UVIS stellar occultations. *Icarus* **216**, 507–534 (2011).
23. M. J. Loeffler, U. Raut, R. A. Baragiola, Radiation chemistry in ammonia-water ices. *J. Chem. Phys.* **132**, 054508 (2010).

24. W. Zheng, D. Jewitt, Y. Osamura, R. I. Kaiser, Formation of nitrogen and hydrogen-bearing molecules in solid ammonia and implications for solar system and interstellar ices. *Astrophys. J.* **674**, 1242–1250 (2008).
25. V. De La Haye, J. H. Waite Jr., R. E. Johnson, R. V. Yelle, T. E. Cravens, J. G. Luhmann, W. T. Kasprzak, D. A. Gell, B. Magee, F. Leblanc, M. Michael, S. Jurac, I. P. Robertson, Cassini ion and neutral mass spectrometer data in Titan's upper atmosphere and exosphere: Observation of a suprathermal corona. *J. Geophys. Res. Space Physics* **112**, A07309 (2007).
26. N. J. Mason, A. Dawes, P. D. Holtom, R. J. Mukerji, M. P. Davis, B. Sivaraman, R. I. Kaiser, S. V. Hoffmann, D. A. Shaw, VUV spectroscopy and photo-processing of astrochemical ices: An experimental study. *Faraday Discuss.* **133**, 311–329 (2006).
27. L. W. Esposito, C. A. Barth, J. E. Colwell, G. M. Lawrence, W. E. McClintock, A. I. F. Stewart, H. U. Keller, A. Korth, H. Lauche, M. C. Festou, A. L. Lane, C. J. Hansen, J. N. Maki, R. A. West, H. Jahn, R. Reulke, K. Warlich, D. E. Shemansky, Y. L. Yung, The Cassini Ultraviolet Imaging Spectrograph Investigation. *Space Sci. Rev.* **115**, 299–361 (2004).
28. W. E. McClintock, G. J. Rottman, T. N. Woods, Paper presented at the Proceedings—SPIE The International Society for Optical Engneering, 2000.
29. R. G. Bhuin, B. Sivaraman, J.-I. Lo, B. N. R. Sekhar, B.-M. Cheng, T. Pradeep, N. J. Mason, Communication: Vacuum ultraviolet photoabsorption of interstellar icy thiols. *J. Chem. Phys.* **141**, 231101 (2014).
30. G. A. Cruz-Diaz, G. M. M. Caro, Y.-J. Chen, Vacuum-UV absorption spectroscopy of interstellar ice analogues. III. Isotopic effects. *Mon. Notices R. Astron. Soc.* **439**, 2370–2376 (2014).
31. A. Dawes, R. J. Mukerji, M. P. Davis, P. D. Holtom, S. M. Webb, B. Sivaraman, S. V. Hoffmann, D. A. Shaw, N. J. Mason, Morphological study into the temperature dependence of solid ammonia under astrochemical conditions using vacuum ultraviolet and Fourier-transform infrared spectroscopy. *J. Chem. Phys.* **126**, 244711 (2007).
32. A. Dawes, N. Pascual, S. V. Hoffmann, N. C. Jones, N. J. Mason, Vacuum ultraviolet photoabsorption spectroscopy of crystalline and amorphous benzene. *Phys. Chem. Chem. Phys.* **19**, 27544–27555 (2017).
33. A. Dawes, N. Pascual, N. J. Mason, S. Gärtner, S. V. Hoffmann, N. C. Jones, Probing the interaction between solid benzene and water using vacuum ultraviolet and infrared spectroscopy. *Phys. Chem. Chem. Phys.* **20**, 15273–15287 (2018).
34. S. Pavithraa, J.-I. Lo, K. Rahul, B. N. Raja Sekhar, B.-M. Cheng, N. J. Mason, B. Sivaraman, Vacuum ultraviolet photoabsorption of prime ice analogues of Pluto and Charon. *Spectrochim. Acta A Mol. Biomol. Spectrosc.* **190**, 172–176 (2018).
35. S. Pavithraa, D. Sahu, G. Seth, J.-I. Lo, B. N. Raja Sekhar, B.-M. Cheng, A. Das, N. J. Mason, B. Sivaraman, SH stretching vibration of propanethiol ice—A signature for its identification in the interstellar icy mantles. *Astrophys. Space Sci.* **362**, 126 (2017).
36. B. Sivaraman, B. G. Nair, B. N. Raja Sekhar, J.-I. Lo, R. Sridharan, B.-M. Cheng, N. J. Mason, Vacuum ultraviolet photoabsorption of pure solid ozone and its implication on the identification of ozone on Moon. *Chem. Phys. Lett.* **603**, 33–36 (2014).
37. B. Sivaraman, S. Pavithraa, J.-I. Lo, B. N. R. Sekhar, H. Hill, B.-M. Cheng, N. J. Mason, Vacuum ultraviolet photoabsorption spectra of nitrile ices for their identification on Pluto. *Astrophys. J.* **825**, 141 (2016).
38. B. Sivaraman, B. N. Raja Sekhar, N. C. Jones, S. V. Hoffmann, N. J. Mason, VUV spectroscopy of formamide ices. *Chem. Phys. Lett.* **554**, 57–59 (2012).
39. S. G. Warren, Optical constants of ice from the ultraviolet to the microwave. *Appl. Optics* **23**, 1206–1225 (1984).
40. B. Hapke, *Theory of Reflectance and Emittance Spectroscopy* (Cambridge Univ. Press, ed. 2, 2012).

Acknowledgments: We would like to express our thanks to the Cassini Team. We acknowledge the help of S. Pavithraa and S. P. Murali Babu (NCTU, Taiwan) during the course of the experiments. B.S., B.N.R.S., and N.J.M. acknowledge the effort of B. Vaishnav and D. Mehta, PRL, in bringing up the ACID database. **Funding:** B.S. and N.J.M. would like to thank the support from Sir John and Lady Mason Academic Trust, NSRRC (Taiwan), University of Kent (UK), and The Open University (UK). B.S., N.J.M., J.-I.L., B.N.R.S., and B.-M.C. recognize the VUV beamtime support from NSRRC (Taiwan). B.S. acknowledges the support from Inspire grant (IFA-11CH-11) as part of this work was carried out during 2012–2017 and the Physical Research Laboratory (PRL), Department of Space (Government of India). **Author contributions:** M.E. carried out the Cassini data reduction. B.S. planned and coordinated the experiments. B.S., J.-I.L., S.-L.C., B.-M.C., B.N.R.S., and N.J.M. constitute the experimental team. M.E., A.H., B.S., and N.J.M. carried out the analysis. All the authors contributed to the manuscript. **Competing interests:** The authors declare that they have no competing interests. **Data and materials availability:** Experimental data presented in this manuscript can be accessed at www.prl.res.in/~dinesh/acid. All data needed to evaluate the conclusions in the paper are present in the paper and/or the Supplementary Materials. Additional data related to this paper may be requested from the authors.

Submitted 14 December 2019
Accepted 18 November 2020
Published 22 January 2021
10.1126/sciadv.aba5749

Citation: M. Elowitz, B. Sivaraman, A. Hendrix, J.-I. Lo, S.-L. Chou, B.-M. Cheng, B. N. R. Sekhar, N. J. Mason, Possible detection of hydrazine on Saturn's moon Rhea. *Sci. Adv.* **7**, eaba5749 (2021).

Possible detection of hydrazine on Saturn's moon Rhea

Mark Elowitz, Bhalamurugan Sivaraman, Amanda Hendrix, Jen-Iu Lo, Sheng-Lung Chou, Bing-Ming Cheng, B. N. Raja Sekhar and Nigel J. Mason

Sci Adv **7** (4), eaba5749.
DOI: 10.1126/sciadv.aba5749